8

Design Charts for Finite-Length Journal Bearings

8.1 INTRODUCTION

In the preceding chapters, the analysis of infinitely long and short journal bearings have been presented. In comparison, the solution of a finite-length journal bearing (e.g., $L/D = 1$) is more complex and requires a computer program for a numerical solution of the Reynolds equation. The first numerical solution of the Reynolds equation for a finite-length bearing was performed by Raimondi and Boyd (1958). The results were presented in the form of dimensionless charts and tables, which are required for journal bearing design. The presentation of the results in the form of dimensionless charts and tables is convenient for design purposes because one does not need to repeat the numerical solution for each bearing design. The charts and tables present various dimensionless *performance parameters*, such as minimum film thickness, friction, and temperature rise of the lubricant as a function of the Sommerfeld number, S. Let us recall that the dimensionless Sommerfeld number is defined as

$$S = \left(\frac{R}{C}\right)^2 \frac{\mu n}{P} \tag{8-1}$$

where n is the speed of the journal in revolutions per second (RPS), R is the journal radius, C is the radial clearance, and P is the average bearing pressure (load, F, per unit of projected contact area of journal and bearing), given by

$$P = \frac{F}{2RL} = \frac{F}{DL} \tag{8-2}$$

Note that S is a dimensionless number, and any system of units can be applied for its calculation as long as one is consistent with the units. For instance, if the Imperial unit system is applied, length should be in inches, force in lbf, and μ in reynolds [lbf-s/in.^{2}]. In SI units, length is in meters, force in newtons, and the viscosity, μ, in [N-s/m^2]. The journal speed, n, should always be in revolutions per second (RPS), irrespective of the system of units used, and the viscosity, μ, must always include seconds as the unit of time.

8.2 DESIGN PROCEDURE

The design procedure starts with the selection of the bearing dimensions: the journal diameter D, the bearing length L, and the radial clearance between the bearing and the journal C. At this stage of the design, the shaft diameter should already have been computed according to strength-of-materials considerations. However, in certain cases the designer may decide, after preliminary calculations, to increase the journal diameter in order to improve the bearing hydrodynamic load capacity.

One important design decision is the selection of the L/D ratio. It is obvious from hydrodynamic theory of lubrication that a long bearing has a higher load capacity (per unit of length) in comparison to a shorter bearing. On the other hand, a long bearing increases the risk of bearing failure due to misalignment errors. In addition, a long bearing reduces the amount of oil circulating in the bearing, resulting in a higher peak temperature inside the lubrication film and the bearing surface. Therefore, short bearings (L/D ratios between 0.5 and 0.7) are recommended in many cases. Of course, there are many unique circumstances where different ratios are selected.

The bearing clearance, C, is also an important design factor, because the load capacity in a long bearing is proportional to $(R/C)^2$. Experience over the years has resulted in an empirical rule used by most designers. They commonly select a ratio R/C of about 1000. The ratio R/C is equal to the ratio $D/\Delta D$ between the diameter and the diameter clearance; i.e., a journal of 50-mm diameter should have a 50-μm (fifty-thousandth of a millimeter)-diameter clearance. The designer should keep in mind that there are manufacturing tolerances of bearing bore and journal diameters, resulting in significant tolerances in the journal bearing clearance, ΔD. The clearance can be somewhat smaller or larger, and thus the bearing should be designed for the worst possible

scenario. In general, high-precision manufacturing is required for journal bearings, to minimize the clearance tolerances as well as to achieve good surface finish and optimal alignment.

For bearings subjected to high dynamic impacts, or very high speeds, somewhat larger bearing clearances are chosen. The following is an empirical equation that is recommended for high-speed journal bearings having an L/D ratio of about 0.6:

$$\frac{C}{D} = (0.0009 + \frac{n}{83{,}000}) \tag{8-3}$$

where n is the journal speed (RPS). This equation is widely used to determine the radial clearance in motor vehicle engines.

8.3 MINIMUM FILM THICKNESS

One of the most critical design decisions concerns the minimum film thickness, h_n. Of course, the minimum fluid film thickness must be much higher than the surface roughness, particularly in the presence of vibrations. Even for statically loaded bearings, there are always unexpected disturbances and dynamic loads, due to vibrations in the machine, and a higher value of the minimum film thickness, h_n, is required to prevent bearing wear. In critical applications, where the replacement of bearings is not easy, such as bearings located inside an engine, more care is required to ensure that the minimum film thickness will never be reduced below a critical value at which wear can initiate.

Another consideration is the fluid film temperature, which can increase under unexpected conditions, such as disturbances in the operation of the machine. The temperature rise reduces the lubricant viscosity; in turn, the oil film thickness is reduced. For this reason, designers are very careful to select h_n much larger than the surface roughness. The common design practice for hydrodynamic bearings is to select a minimum film thickness in the range of 10–100 times the average surface finish (in RMS). For instance, if the journal and the bearing are both machined by fine turning, having a surface finish specified by an RMS value of 0.5 μm (0.5 thousandths of a millimeter), the minimum film thickness can be within the limits of 5–50 μm. High h_n values are chosen in the presence of high dynamic disturbances, whereas low values of h_n are chosen for steady operation that involves minimal vibrations and disturbances.

Moreover, if it is expected that dust particles would contaminate the lubricant, a higher minimum film thickness, h_n, should be selected. Also, for critical applications, where there are safety considerations, or where bearing failure can result in expensive machine downtime, a coefficient of safety is applied in the form of higher values of h_n.

The surface finish of the two surfaces (bearing and journal) must be considered. A dimensionless film parameter, Λ, relating h_n to the average surface finish, has been introduced; see Hamrock (1994):

$$\Lambda = \frac{h_n}{(R_{s,j}^2 + R_{s,b}^2)^{1/2}} \tag{8-4}$$

where $R_{s,j}$ = surface finish of the journal surface (RMS) and $R_{s,b}$ = surface finish of the bearing surface (RMS).

As discussed earlier, the range of values assigned to Λ depends on the operating conditions and varies from 5 to 100. The minimum film thickness is not the only limitation encountered in the design of a journal bearing. Other limitations, which depend on the bearing material, determine in many cases the maximum allowable bearing load. The most important limitations are as follows.

1. Maximum allowed PV value (depending on the bearing material) to avoid bearing overheating during the start-up of boundary lubrication. This is particularly important in bearing materials that are not good heat conductors, such as plastics materials.
2. Maximum allowed peak pressure to prevent local failure of the bearing material.
3. Maximum allowed peak temperature, to prevent melting or softening of the bearing material.

In most applications, the inner bearing surface is made of a thin layer of a soft white metal (babbitt), which has a low melting temperature. The design procedure must ensure that the allowed values are not exceeded, for otherwise it can result in bearing failure. If the preliminary calculations indicate that these limitations are exceeded, it is necessary to introduce design modifications. In most cases, the design of hydrodynamic bearing requires trial-and-error calculations to verify that all the requirements are satisfied.

8.4 RAIMONDI AND BOYD CHARTS AND TABLES

8.4.1 Partial Bearings

A partial journal bearing has a bearing arc, β, of less than 360°, and only part of the bearing circumference supports the journal. A full bearing is where the bearing arc $\beta = 360^\circ$; in a partial bearing, the bearing arc is less than 360°, such as $\beta = 60^\circ$, 120°, and 180°. A partial bearing has two important advantages in comparison to a full bearing. First, there is a reduction of the viscous friction coefficient; second, in a partial bearing there is a faster circulation of the lubricant, resulting in better heat transfer from the bearing. The two advantages

result in a lower bearing temperature as well as lower energy losses from viscous friction. In high-speed journal bearings, the friction coefficient can be relatively high, and partial bearings are often used to mitigate this problem. At the same time, the load capacity of a partial bearing is only slightly below that of a full bearing, which make the merits of using a partial bearing quite obvious.

8.4.2 Dimensionless Performance Parameters

Using numerical analysis, Raimondi and Boyd solved the Reynolds equation. They presented the results in dimensionless terms via graphs and tables. Dimensionless performance parameters of a finite-length bearing were presented as a function of the Sommerfeld number, S. The Raimondi and Boyd performance parameters are presented here by charts for journal bearings with the ratio $L/D = 1$; see Figs. 8-1 to 8-10. For bearings having different L/D ratios, the performance parameters are given in tables; see Tables 8-1 to 8-4.

The charts and tables of Raimondi and Boyd have been presented for both partial and full journal bearings, and for various L/D ratios. Partial journal bearings include multi-lobe bearings that are formed by several eccentric arcs.

The following ten dimensionless performance parameters are presented in charts and tables.

1. Minimum film thickness ratio, h_n/C. Graphs of minimum film thickness ratio versus Sommerfeld number, S, are presented in Fig. 8-1.
2. Attitude angle, ϕ, i.e., the angle at which minimum film thickness is attained. The angle is measured from the line along the load direction as shown in Fig. 8-2.
3. Friction coefficient variable, $(R/C)f$. Curves of the dimensionless friction coefficient variable versus S are presented in Fig. 8-3.
4. In Fig. 8-4, curves are plotted of the dimensionless total bearing flow rate variable, $Q/nRCL$, against the Sommerfeld number.
5. The ratio of the side flow rate (in the z direction) to the total flow rate, Q_s/Q, as a function of the Sommerfeld number is shown in Fig. 8-5. The side flow rate, Q_s, is required for determining the end leakage, since the bearing is no longer assumed to be infinite. The side flow rate is important for cooling of the bearing.
6. The dimensionless temperature rise variable, $c\rho\Delta T/P$, is presented in Fig. 8-6. It is required for determining the temperature rise of the lubricant due to friction. The temperature rise, ΔT, is of the lubricant from the point of entry into the bearing to the point of discharge from the bearing. The estimation of the temperature rise is discussed in greater detail later.

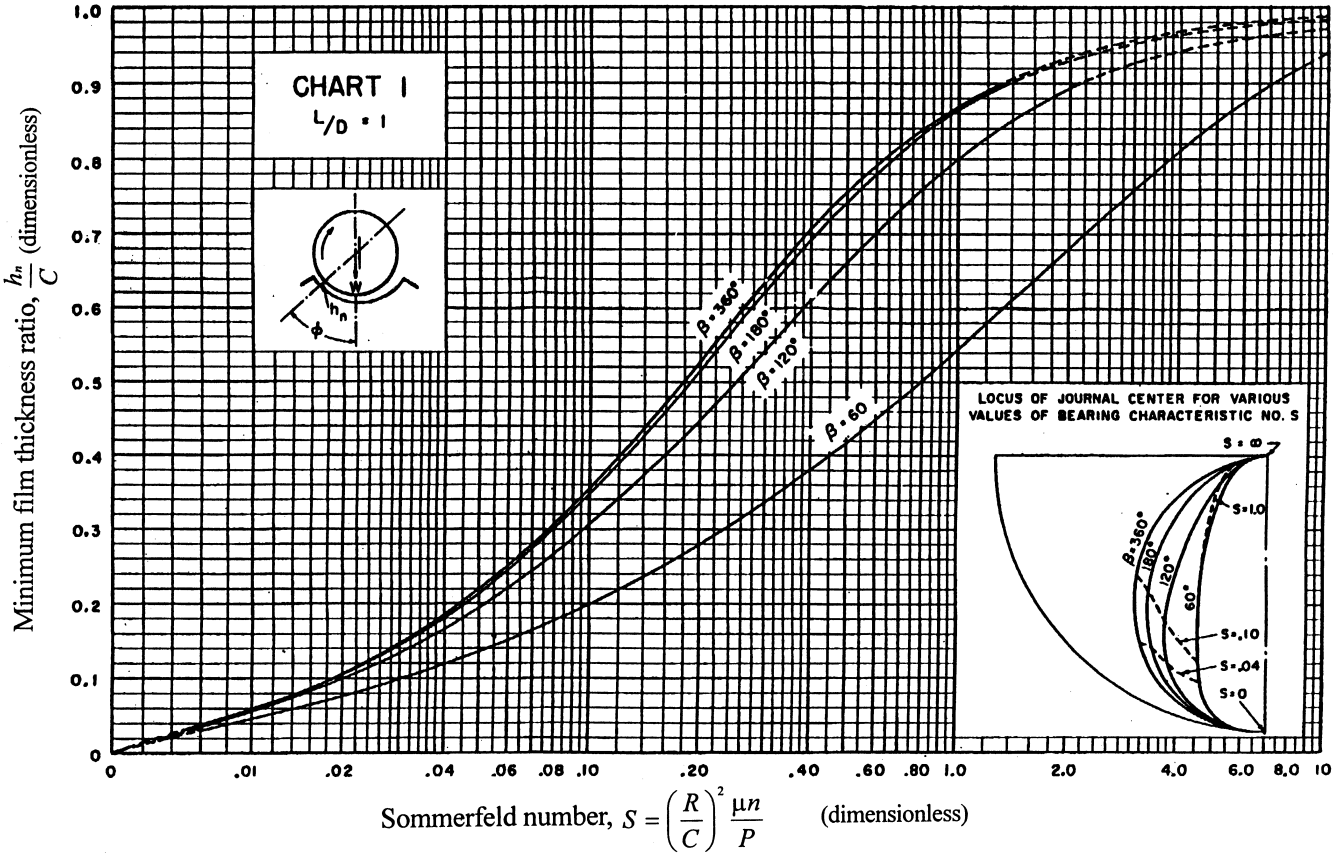

FIG. 8-1 Minimum film thickness ratio versus Sommerfeld number for variable bearing arc β, $L/D = 1$. (From Raimondi and Boyd, 1958, with permission of STLE.)

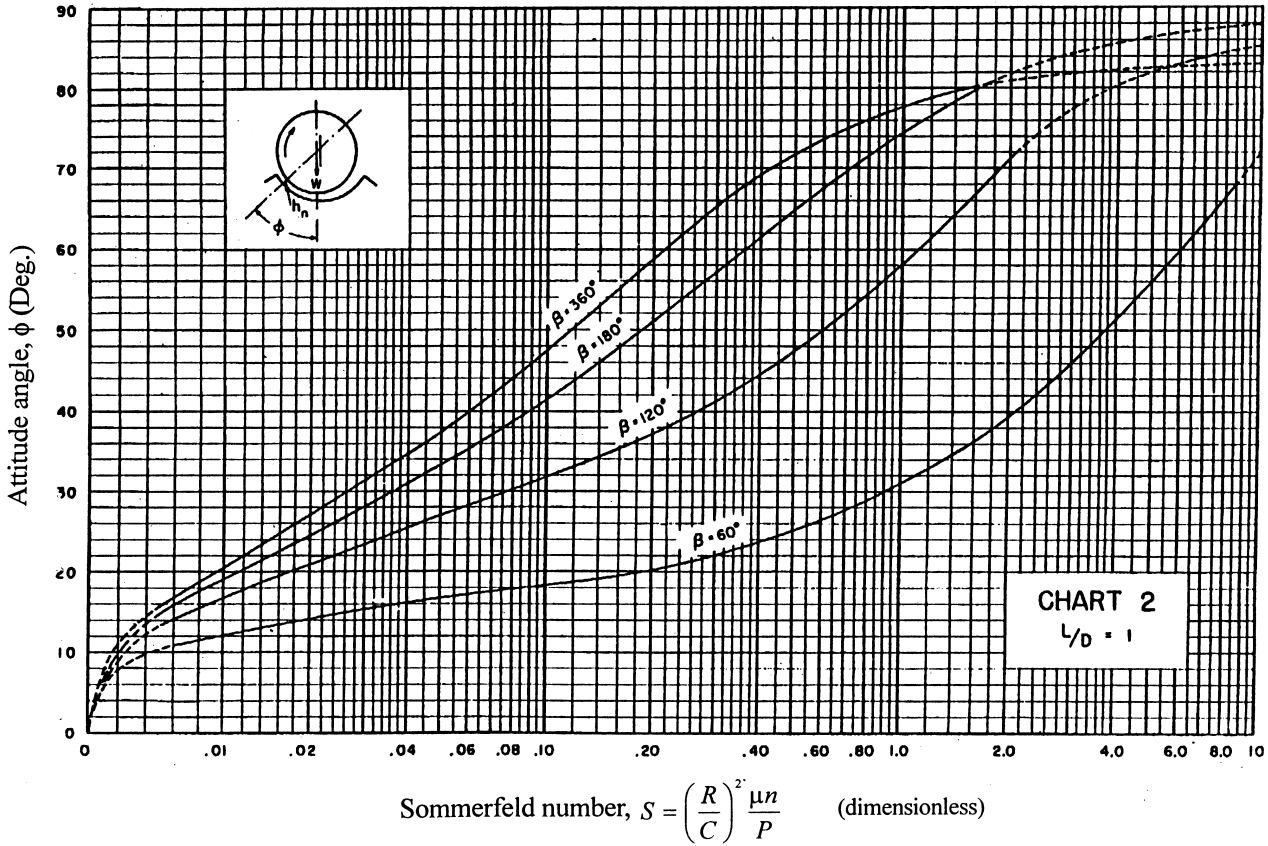

FIG. 8-2 Attitude angle versus Sommerfeld number for variable bearing arc β, $L/D = 1$. (From Raimondi and Boyd, 1958, with permission of STLE.)

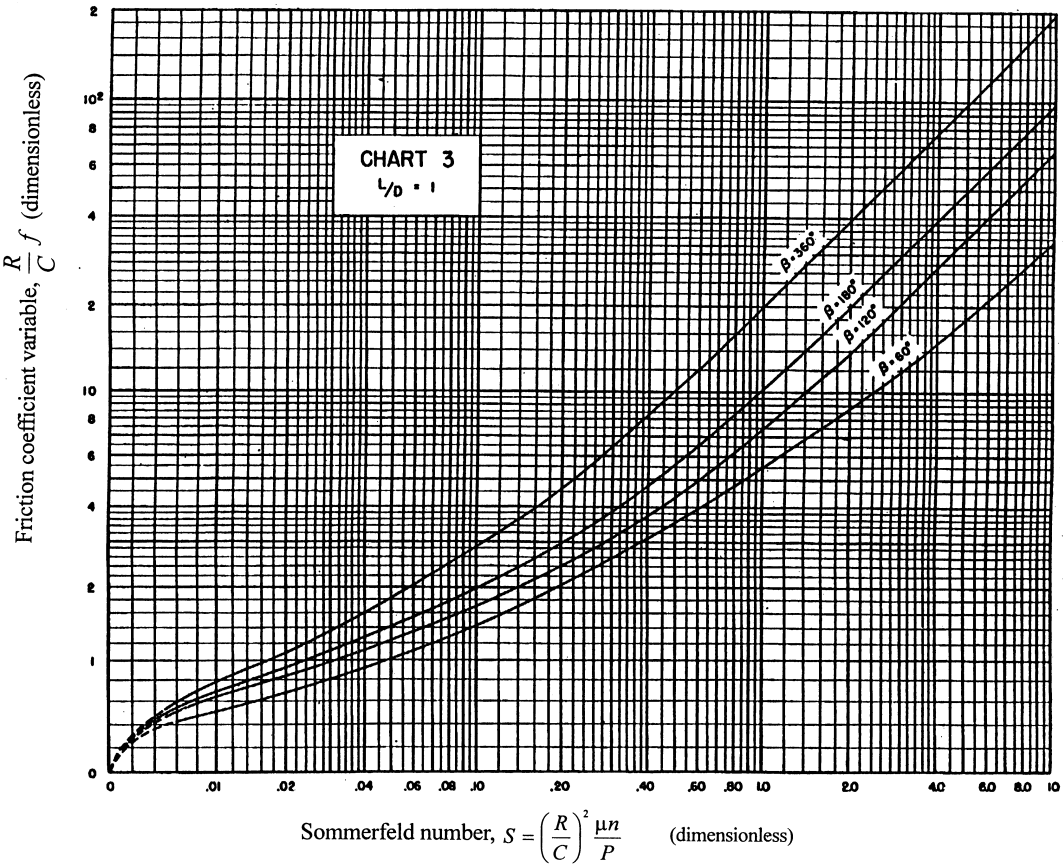

FIG. 8-3 Friction coefficient versus Sommerfeld number for variable bearing arc β, $L/D = 1$. (From Raimondi and Boyd, 1958, with permission of STLE.)

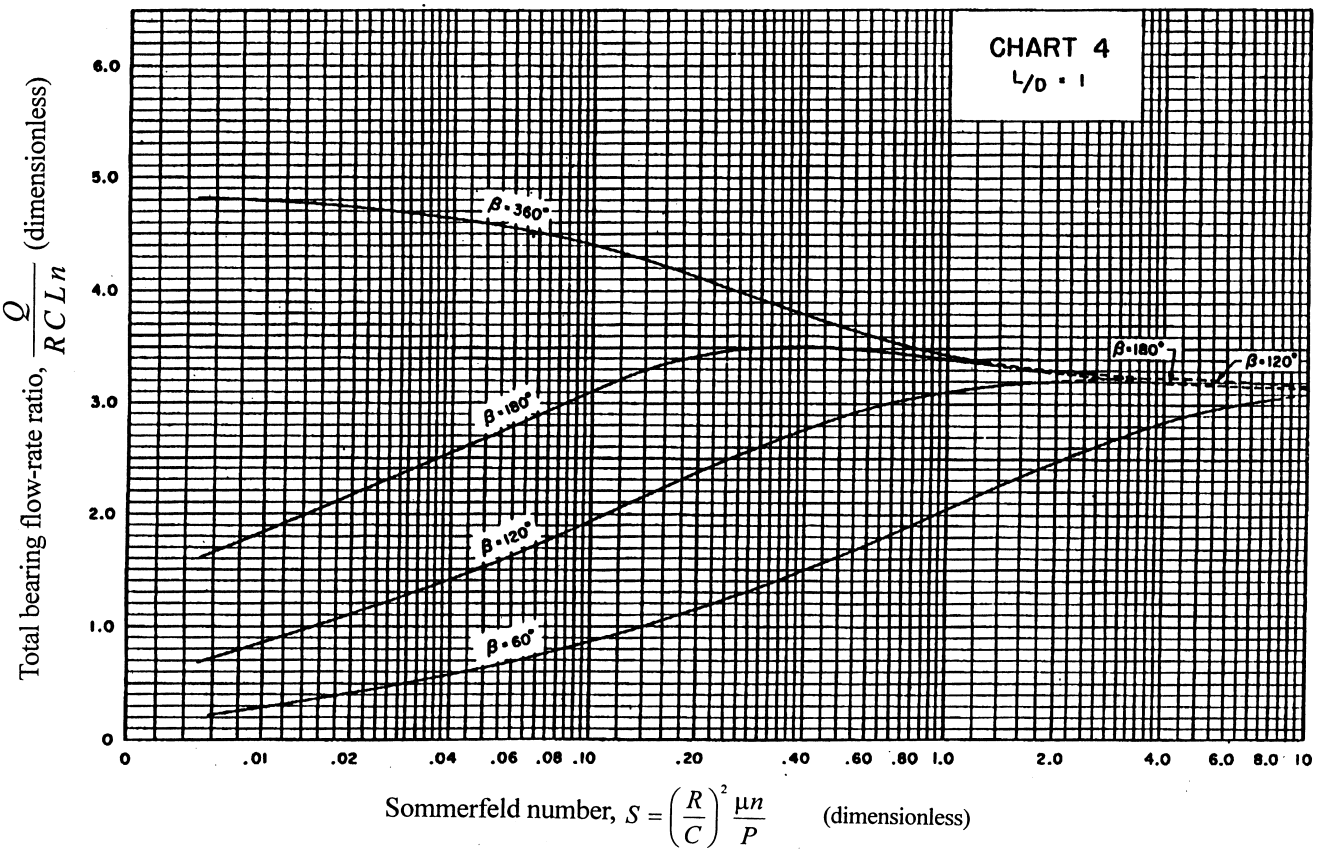

FIG. 8-4 Total bearing flow rate variable versus Sommerfeld number, ($L/D = 1$). (From Raimondi and Boyd, 1958, with permission of STLE.)

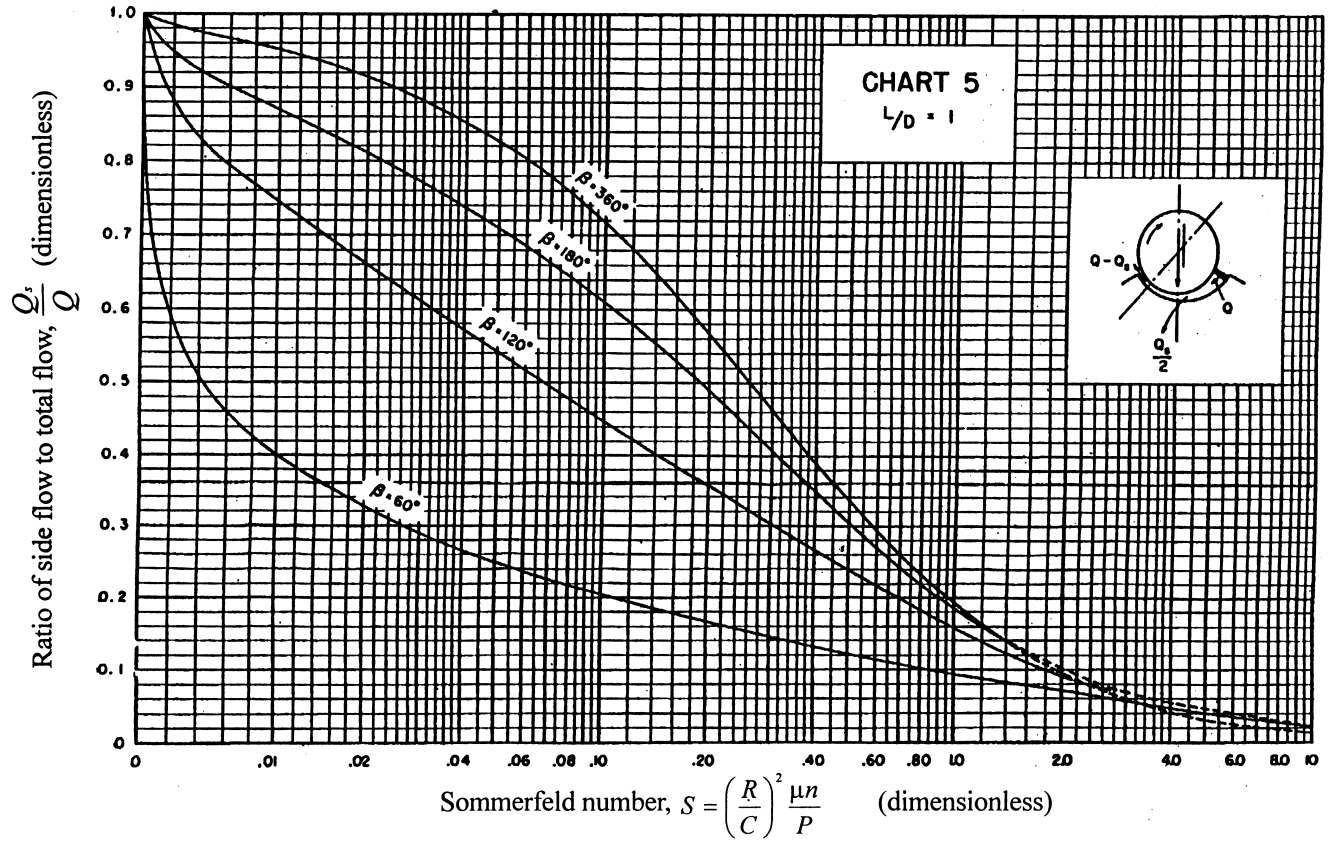

FIG. 8-5 Ratio of side flow (axial direction) to total flow versus Sommerfeld number ($L/D = 1$). (From Raimondi and Boyd, 1958, with permission of STLE.)

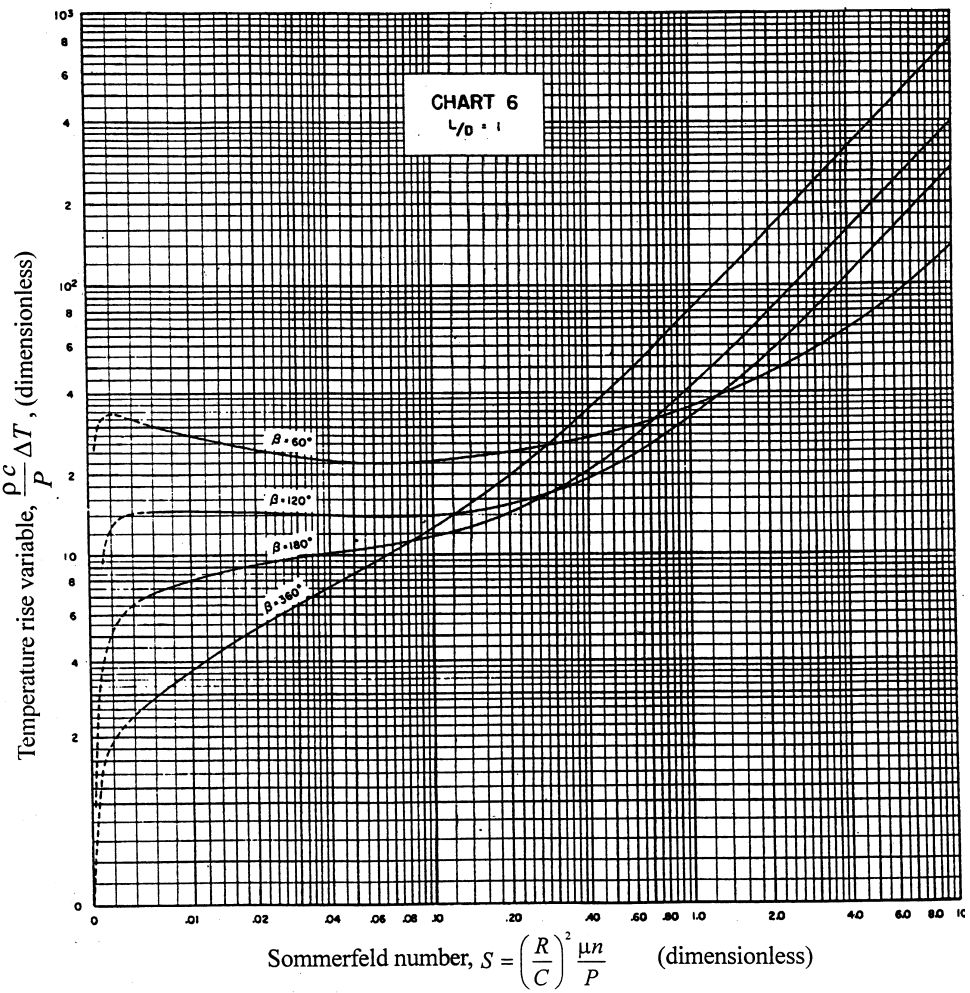

FIG. 8-6 Temperature rise variable versus Sommerfeld number ($L/D = 1$). (From Raimondi and Boyd, 1958, with permission of STLE.)

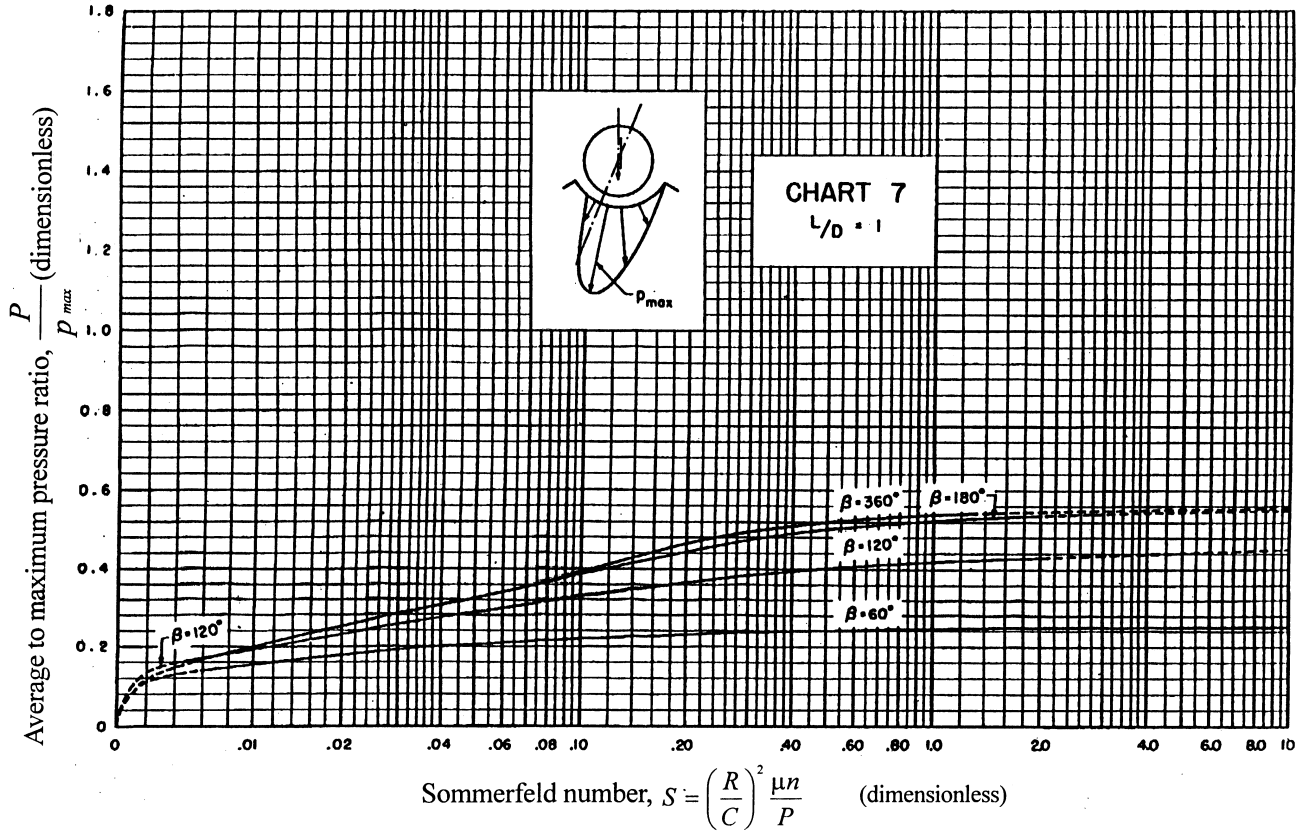

FIG. 8-7 Average to maximum pressure ratio versus Sommerfeld number ($L/D = 1$). (From Raimondi and Boyd, 1958, with permission of STLE.)

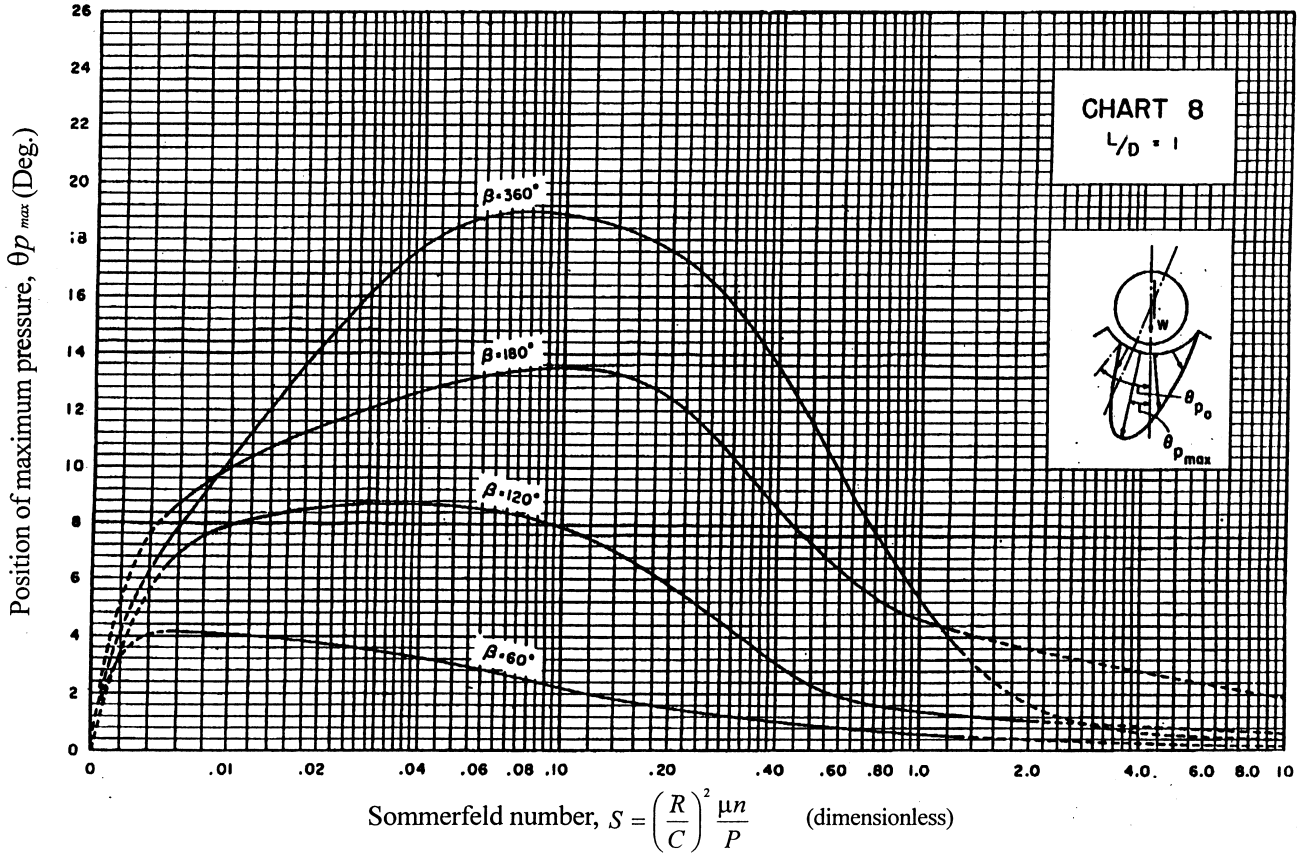

FIG. 8-8 Position of maximum pressure versus Sommerfeld number ($L/D = 1$). (From Raimondi and Boyd, 1958, with permission of STLE.)

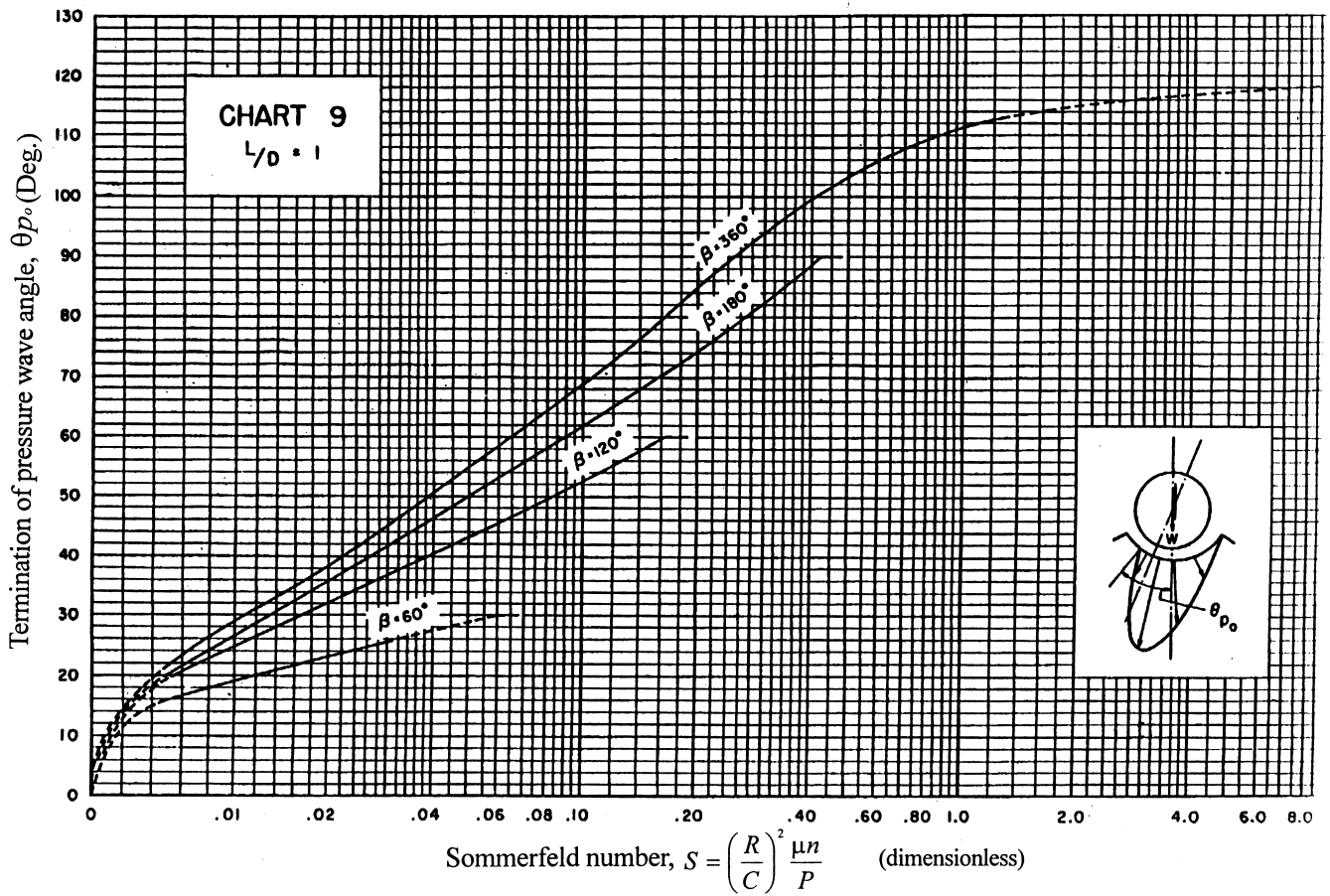

FIG. 8-9 Termination of pressure wave angle versus Sommerfeld number ($L/D = 1$). (From Raimondi and Boyd, 1958, with permission of STLE.)

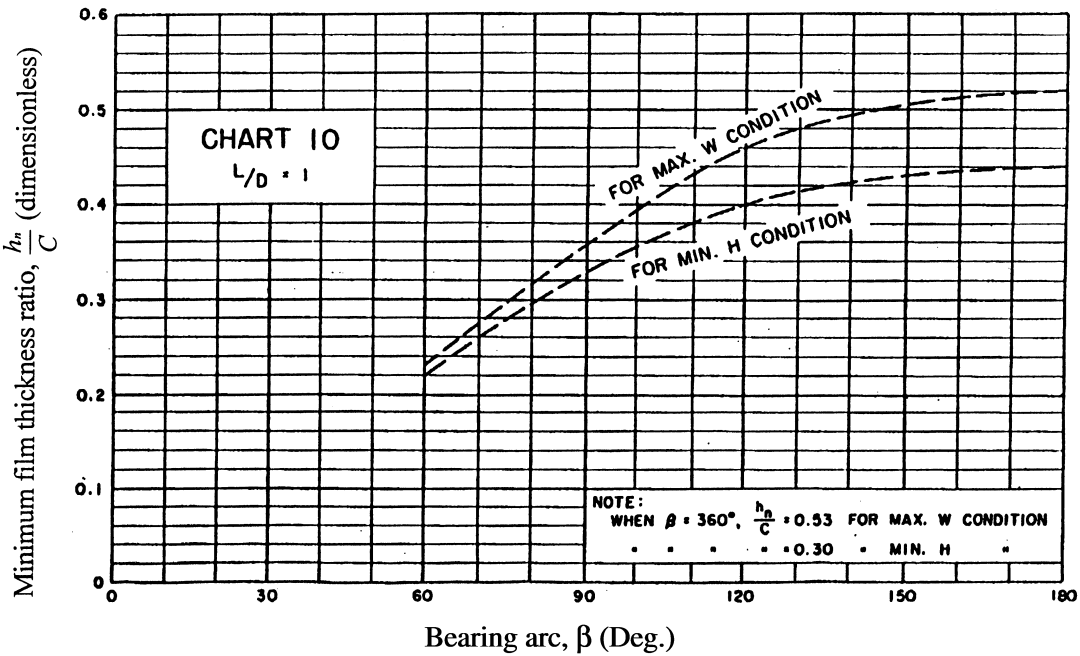

FIG. 8-10 Chart for determining the value of the minimum film thickness versus bearing arc for maximum load, and minimum power loss ($L/D = 1$). (From Raimondi and Boyd, 1958, with permission of STLE.)

TABLE 8-1 Performance Characteristics for a Centrally Loaded 360° Bearing

$\frac{L}{D}$	ε	$\frac{h_n}{C}$	θ_A	$\frac{\alpha}{\beta}$	S	ϕ	$\frac{R}{C}f$	$\frac{Q}{nRCL}$	$\frac{Q_s}{Q}$	$\frac{\rho c}{P}\Delta T$	$\frac{P}{p_{max}}$	$\theta_{p_{max}}$	θ_{p_0}
∞	0	1	0	---	∞	70.92	∞	π	0	∞	---	0	149.38
	0.1	0.9	0	0.308	0.24	69.1	4.8	3.03	0	19.9	0.826	0	137
	0.2	0.8	0	0.314	0.123	67.26	2.57	2.83	0	11.4	0.814	5.6	128
	0.4	0.6	0	0.328	0.0626	61.94	1.52	2.26	0	8.47	0.764	14.4	107
	0.6	0.4	0	0.349	0.0389	54.31	1.2	1.56	0	9.73	0.667	20.8	86
	0.8	0.2	0	0.383	0.021	42.22	0.961	0.76	0	15.9	0.495	21.5	58.8
	0.9	0.1	0	0.412	0.0115	31.62	0.756	0.411	0	23.1	0.358	19	44
	0.97	0.03	0	---	---	---	---	---	0	---	---	---	---
	1	0	0	---	0	0	0	0	0	□□	0	0	0
1	0	1	0	---	∞	85	∞	π	0	∞	---	0	119
	0.1	0.9	0	0.279	1.33	79.5	26.4	3.37	0.15	106	0.54	3.5	113
	0.2	0.8	0	0.294	0.631	74.02	12.8	3.59	0.28	52.1	0.529	9.2	106
	0.4	0.6	0	0.325	0.264	63.1	5.79	3.99	0.497	24.3	0.484	16.5	91.2
	0.6	0.4	0	0.36	0.121	50.58	3.22	4.33	0.68	14.2	0.415	18.7	72.9
	0.8	0.2	0	0.399	0.0446	36.24	1.7	4.62	0.842	8	0.313	18.2	52.3
	0.9	0.1	0	0.426	0.0188	26.45	1.05	4.74	0.919	5.16	0.247	13.8	37.3
	0.97	0.03	0	0.457	0.00474	15.47	0.514	4.82	0.973	2.61	0.152	7.1	20.5
	1	0	0	---	0	0	0	---	1	0	0	0	0
0.5000	0	1	0	---	∞	88.5	∞	π	0	∞	---	0	107
	0.1	0.9	0	0.273	4.31	81.62	85.6	3.43	0.173	343	0.523	5.8	99.2
	0.2	0.8	0	0.292	2.03	74.97	40.9	3.72	0.318	164	0.506	11.9	92.5
	0.4	0.6	0	0.329	0.779	61.45	17	4.29	0.552	68.6	0.441	16.9	78.8
	0.6	0.4	0	0.366	0.319	48.14	8.1	4.85	0.73	33	0.365	17.1	64.3
	0.8	0.2	0	0.408	0.0923	33.31	3.26	5.41	0.874	13.4	0.267	15.3	44.2
	0.9	0.1	0	0.434	0.0313	23.66	1.6	5.69	0.939	6.66	0.206	11	33.8
	0.97	0.03	0	0.462	0.00609	13.75	0.61	5.88	0.98	2.56	0.126	3.8	19.1
	1	0	0	---	0	0	0	---	1	0	0	0	0
0.2500	0	1	0	---	∞	89.5	∞	π	0	∞	---	0	99
	0.1	0.9	0	0.271	16.2	82.31	322	3.45	0.18	1287	0.515	7.4	98.9
	0.2	0.8	0	0.291	7.57	75.18	153	3.76	0.33	611	0.489	13.5	85
	0.4	0.6	0	0.331	2.83	60.86	61.2	4.37	0.567	245	0.415	17.4	70
	0.6	0.4	0	0.37	1.07	46.72	26.7	4.99	0.746	107	0.334	16.4	55.5
	0.8	0.2	0	0.414	0.261	31.04	8.8	5.6	0.884	35.4	0.24	11.5	39.7
	0.9	0.1	0	0.439	0.0736	21.85	3.5	5.91	0.945	14.1	0.18	8.6	27.8
	0.97	0.03	0	0.466	0.0101	12.22	0.922	6.12	0.984	3.73	0.108	4	17.7
	1	0	0	---	0	0	0	---	1	0	0	0	0

TABLE 8-2 Performance Characteristics for a Centrally Loaded 180° Bearing

$\frac{L}{D}$	ε	$\frac{h_n}{C}$	θ_A	$\frac{\alpha}{\beta}$	S	ϕ	$\frac{R}{C}f$	$\frac{Q}{nRCL}$	$\frac{Q_s}{Q}$	$\frac{\rho c}{P}\Delta T$	$\frac{P}{p_{max}}$	$\theta_{p_{max}}$	θ_{p_0}
∞	0	1	0	0.5	∞	90.00	∞	π	0	∞	----	0.0	90.0
	0.10	0.90	17.00	0.5	0.347	72.90	3.550	3.040	0	14.70	0.778	1.6	90.0
	0.20	0.80	28.60	0.5	0.179	61.32	2.010	2.800	0	8.99	0.759	3.4	90.0
	0.40	0.60	40.00	0.5	0.0898	49.99	1.290	2.200	0	7.34	0.700	7.7	90.0
	0.60	0.40	46.90	0.5	0.0523	43.15	1.060	1.520	0	8.71	0.607	12.3	71.8
	0.80	0.20	56.70	0.5	0.0253	33.35	0.859	0.767	0	14.10	0.459	13.7	51.2
	0.90	0.10	64.20	0.501	0.0128	25.57	0.681	0.380	0	22.50	0.337	13.3	36.8
	0.97	0.03	74.65	0.5	0.00384	15.43	0.416	0.119	0	44.00	0.190	9.1	20.7
	1	0	90	1	0	0	0	0	0	∞	0	0	0
1	0	1	0	0.500	∞	90.00	∞	π	0	∞	----	0.0	90.0
	0.10	0.90	11.500	0.500	1.40000	78.50	14.10	3.34	0.139	57.00	0.525	4.5	90.0
	0.20	0.80	21.000	0.500	0.67000	67.93	7.15	3.46	0.252	29.70	0.513	5.9	90.0
	0.40	0.60	34.167	0.500	0.27800	58.86	3.61	3.49	0.425	16.50	0.466	10.8	80.8
	0.60	0.40	45.000	0.502	0.12800	44.67	2.28	3.25	0.572	12.40	0.403	13.4	66.8
	0.80	0.20	58.000	0.498	0.04630	32.33	1.39	2.63	0.721	10.40	0.313	12.9	48.5
	0.90	0.10	66.000	0.499	0.01930	24.14	0.92	2.14	0.818	9.13	0.244	11.3	35.2
	0.97	0.03	75.584	0.499	0.00483	14.57	0.48	1.60	0.915	6.96	0.157	8.2	20.0
	1	0	90	0.5	0	0	0	----	1	0	0	0	0
0.5000	0	1	0	0.500	∞	90.00	∞	π	0	∞	----	0.0	90.0
	0.10	0.90	10.0	0.500	4.38000	79.97	44.00	3.41	0.167	177.00	0.518	5.4	90.0
	0.20	0.80	17.8	0.500	2.06000	72.14	21.60	3.64	0.302	87.80	0.499	9.1	90.0
	0.40	0.60	32.0	0.500	0.79400	58.01	9.96	3.93	0.506	42.70	0.438	13.7	71.9
	0.60	0.40	45.0	0.500	0.32100	45.01	5.41	3.93	0.665	25.90	0.365	14.1	59.1
	0.80	0.20	59.0	0.498	0.09210	31.29	2.54	3.56	0.806	15.00	0.273	12.1	43.9
	0.90	0.10	67.2	0.500	0.03140	22.80	1.38	3.17	0.886	9.80	0.208	10.4	31.5
	0.97	0.03	76.5	0.499	0.00625	13.63	0.58	2.62	0.951	5.30	0.132	6.9	18.1
	1	0	90	0.5	0	0	0	0	1	0	0	0	0
0.2500	0	1	0	0.5	∞	90.00	∞	π	0	∞	---	0.0	90.0
	0.10	0.9251	9.0	0.498	16.3000	81.40	163.00	3.44	0.176	653.0	0.513	6.3	90.0
	0.20	0.8242	16.3	0.500	7.6000	73.70	79.40	3.71	0.32	320.0	0.489	12.4	80.9
	0.40	0.6074	31.0	0.500	2.8400	58.99	35.10	4.11	0.534	146.0	0.417	15.8	70.5
	0.60	0.4000	45.0	0.500	1.0800	44.96	17.60	4.25	0.698	79.8	0.336	14.8	53.6
	0.80	0.2000	59.3	0.502	0.2630	30.43	6.88	4.07	0.837	36.5	0.241	11.4	39.0
	0.90	0.1000	68.9	0.498	0.0736	21.43	2.99	3.72	0.905	18.4	0.180	9.3	27.3
	0.97	0.0300	77.7	0.500	0.0104	12.28	0.88	3.29	0.961	6.5	0.110	6.3	17.5
	1	0	90.0	0.500	0	0	0	---	1	0	0	0	0

TABLE 8-3 Performance Characteristics for a Centrally Loaded 120° Bearing

$\frac{L}{D}$	ε	$\frac{h_n}{C}$	θ_A	$\frac{\alpha}{\beta}$	S	ϕ	$\frac{R}{C}f$	$\frac{Q}{nRCL}$	$\frac{Q_s}{Q}$	$\frac{\rho c}{P}\Delta T$	$\frac{P}{p_{max}}$	$\theta_{p_{max}}$	θ_{p_0}
∞	0.0000	1.0000	30.0000	0.5000	∞	90.0000	∞	π	0.0000	∞	---	0.0000	60.0000
	0.1000	0.9007	53.3000	0.5000	0.8770	66.6900	6.0200	3.0200	0.0000	25.1000	0.6100	0.4000	60.0000
	0.2000	0.8000	67.4000	0.5000	0.4310	52.6000	3.2600	2.7500	0.0000	14.9000	0.5990	0.9000	60.0000
	0.4000	0.6000	81.0000	0.5000	0.1810	39.0200	1.7800	2.1300	0.0000	10.5000	0.5660	2.4000	60.0000
	0.6000	0.4000	87.3000	0.5000	0.0845	32.6700	1.2100	1.4700	0.0000	10.3000	0.5090	5.1000	60.0000
	0.8000	0.2000	93.2000	0.5000	0.0328	26.8000	0.8530	0.7590	0.0000	14.1000	0.4050	8.2000	44.2000
	0.9000	0.1000	98.5000	0.5000	0.0147	21.5100	0.6530	0.3880	0.0000	21.2000	0.3110	8.7000	32.9000
	0.9700	0.0300	106.1500	0.5000	0.0041	13.8600	0.3990	0.1180	0.0000	42.4000	0.1990	6.6000	19.6000
	1.0000	0.0000	120.0000	0.5000	0.0000	0.0000	0.0000	0.0000	0.0000		0.0000	0.0000	0.0000
1.0000	0.0000	1.0000	30.0000	0.5000	∞	90.0000	∞	π	0.0000	∞	---	0.0000	60.0000
	0.1000	0.9024	47.5000	0.5000	2.1400	74.9900	14.5000	3.2000	0.0876	59.5000	0.4270	1.1000	60.0000
	0.2000	0.8000	62.0000	0.4980	1.0100	63.3800	7.4400	3.1100	0.1570	32.6000	0.4200	1.3000	60.0000
	0.4000	0.6000	76.0000	0.5000	0.3850	48.0700	3.6000	2.7500	0.2720	19.0000	0.3960	3.2000	60.0000
	0.6000	0.4000	84.5000	0.4990	0.1620	38.5000	2.1600	2.2400	0.3840	15.0000	0.3560	6.5000	60.0000
	0.8000	0.2000	92.6000	0.5000	0.0531	28.0200	1.2700	1.5700	0.5350	13.9000	0.2900	8.6000	43.6000
	0.9000	0.1000	98.6670	0.5000	0.0208	21.0200	0.8550	1.1100	0.6570	14.4000	0.2330	8.5000	32.5000
	0.9700	0.0300	106.5000	0.5000	0.0050	13.0000	0.4610	0.6940	0.8120	14.0000	0.1620	6.3000	19.3000
	1.0000	0.0000	120.0000	0.5000	0.0000	0.0000	0.0000		1.0000	0.0000	0.0000	0.0000	0.0000
0.5000	0.0000	1.0000	30.0000	0.5000	∞	90.0000	∞	π	0.0000	∞	---	0.0000	60.0000
	0.1000	0.9034	45.0000	0.5000	5.4200	74.9900	36.6000	3.2900	0.1240	149.0000	0.4310	1.2000	60.0000
	0.2000	0.8003	56.6500	0.5000	2.5100	63.3800	18.1000	3.3200	0.2250	77.2000	0.4240	2.4000	60.0000
	0.4000	0.6000	72.0000	0.5000	0.9140	48.0700	8.2000	3.1500	0.3860	40.5000	0.3890	4.8000	60.0000
	0.6000	0.4000	81.5000	0.5000	0.3540	38.5000	4.4300	2.8000	0.5300	27.0000	0.3360	8.1000	53.4000
	0.8000	0.2000	92.0000	0.5000	0.0973	28.0200	2.1700	2.1800	0.6840	19.0000	0.2610	9.0000	40.5000
	0.9000	0.1000	99.0000	0.5000	0.0324	21.0200	1.2400	1.7000	0.7870	15.1000	0.2030	8.2000	30.4000
	0.9700	0.0300	107.0000	0.5000	0.0063	13.0000	0.5500	1.1900	0.8990	10.6000	0.1360	6.0000	18.2000
	1.0000	0.0000	120.0000	0.5000	0.0000	0.0000	0.0000	---	1.0000	0.0000	0.0000	0.0000	0.0000
0.2500	0.0000	1.0000	30.0000	0.5000	∞	90.0000	∞	π	0.0000	∞	---	0.0000	60.0000
	0.1000	0.9044	43.0000	0.5000	18.4000	76.9700	124.0000	3.3400	0.1430	502.0000	0.4560	3.0000	60.0000
	0.2000	0.8011	54.0000	0.5000	8.4500	65.9700	60.4000	3.4400	0.2600	254.0000	0.4380	4.8000	60.0000
	0.4000	0.6000	68.8330	0.5000	3.0400	51.2300	26.6000	3.4200	0.4420	125.0000	0.3890	8.4000	60.0000
	0.6000	0.4000	79.6000	0.5000	1.1200	40.4200	13.5000	3.2000	0.5990	75.8000	0.3210	10.4000	48.3000
	0.8000	0.2000	91.5600	0.5000	0.2680	28.3800	5.6500	2.6700	0.7530	42.7000	0.2370	9.4000	35.8000
	0.9000	0.1000	99.4000	0.5000	0.0743	20.5500	2.6300	2.2100	0.8460	25.9000	0.1780	7.8000	26.9000
	0.9700	0.0300	108.0000	0.4990	0.0105	12.1100	0.8320	1.6900	0.9310	11.6000	0.1120	5.5000	17.4000
	1.0000	0.0000	120.0000	0.5000	0.0000	0.0000	0.0000	---	1.0000	0.0000	0.0000	0.0000	0.0000

TABLE 8-4 Performance Characteristics for a Centrally Loaded 60° Bearing

$\frac{L}{D}$	ε	$\frac{h_n}{C}$	θ_A	$\frac{\alpha}{\beta}$	S	ϕ	$\frac{Q}{nRCL}$	$\frac{R}{C}f$	$\frac{Q_s}{Q}$	$\frac{\rho c}{P}\Delta T$	$\frac{P}{p_{max}}$	$\theta_{p_{max}}$	θ_{p_0}
∞	0.0000	1.0000	60.0000	0.5000	∞	90.0000	∞	π	0.0000	∞	----	0.0000	30.0000
	0.1000	0.9191	84.0000	0.5020	5.7500	65.9100	19.7000	3.0100	0.0000	82.3000	0.3370	0.1600	30.0000
	0.2000	0.8109	101.0000	0.5020	2.6600	48.9100	10.1000	2.7300	0.0000	46.5000	0.3360	0.1800	30.0000
	0.4000	0.6002	118.0000	0.5010	0.9310	31.9600	4.6700	2.0700	0.0000	28.4000	0.3290	0.2500	30.0000
	0.6000	0.4000	126.8000	0.5000	0.3220	23.2100	2.4000	1.4000	0.0000	21.5000	0.3170	0.5400	30.0000
	0.8000	0.2000	132.6000	0.5000	0.0755	17.3900	1.1000	0.7220	0.0000	19.2000	0.2870	1.7000	30.0000
	0.9000	0.1000	135.0600	0.5000	0.0241	14.9400	0.6670	0.3720	0.0000	22.5000	0.2430	3.2000	25.5000
	0.9700	0.0300	139.1400	0.5000	0.0050	10.8800	0.3720	0.1150	0.0000	40.7000	0.1630	4.2000	16.9000
	1.0000	0.0000	150.0000	0.5000	0.0000	0.0000	0.0000	0.0000	0.0000	∞	0.0000	0.0000	0.0000
1	0.0000	1.0000	60.0000	0.5000	∞	90.0000	∞	π	0.0000	∞	----	0.0000	30.0000
	0.1000	0.9212	82.0000	0.5010	8.5200	67.9200	29.1000	3.0700	0.0267	121.0000	0.2520	0.3000	30.0000
	0.2000	0.8133	99.0000	0.5010	3.9200	50.9600	14.8000	2.8200	0.4810	67.4000	0.2510	0.3000	30.0000
	0.4000	0.6010	116.0000	0.5000	1.3400	33.9900	6.6100	2.2200	0.0849	39.1000	0.2470	0.5400	30.0000
	0.6000	0.4000	125.5000	0.4990	0.4500	24.5600	3.2900	1.5600	0.1270	28.2000	0.2390	0.9500	30.0000
	0.8000	0.2000	131.6000	0.5010	0.1010	18.3300	1.4200	0.8830	0.2000	22.5000	0.2200	2.2000	30.0000
	0.9000	0.1000	134.6700	0.5000	0.0309	15.3300	0.8220	0.5190	0.2870	23.2000	0.1920	3.5000	25.9000
	0.9700	0.0300	139.1000	0.5000	0.0058	10.8800	0.4220	0.2260	0.4650	30.5000	0.1390	4.2000	16.9000
	1.0000	0.0000	150.0000	0.5000	0.0000	0.0000	0.0000	----	1.0000	0.0000	0.0000	0.0000	0.0000
0.5000	0.0000	1.0000	60.0000	0.5000	∞	90.0000	∞	π	0.0000	∞	---	0.0000	30.0000
	0.1000	0.9223	81.0000	0.5000	14.2000	69.0000	48.6000	3.1100	0.0488	201.0000	0.2390	0.0000	30.0000
	0.2000	0.8152	97.5000	0.4980	6.4700	52.6000	24.2000	2.9100	0.0883	109.0000	0.2390	0.0300	30.0000
	0.4000	0.6039	113.0000	0.5000	2.1400	37.0000	10.3000	2.3800	0.1600	59.4000	0.2330	0.4500	30.0000
	0.6000	0.4000	123.0000	0.5000	0.6950	26.9800	4.9300	1.7400	0.2360	40.3000	0.2250	1.0000	30.0000
	0.8000	0.2000	130.4000	0.5000	0.1490	19.5700	2.0200	1.0500	0.3500	29.4000	0.2010	2.2000	30.0000
	0.9000	0.1000	134.0900	0.5000	0.0422	15.9100	1.0800	0.6640	0.4640	26.5000	0.1720	3.8000	25.4000
	0.9700	0.0300	139.2200	0.4990	0.0070	10.8500	0.4900	0.3290	0.6500	27.8000	0.1220	4.2000	16.6000
	1.0000	0.0000	150.0000	0.5000	0.0000	0.0000	0.0000	----	1.0000	0.0000	0.0000	0.0000	0.0000
0.2500	0.0000	1.0000	60.0000	0.5000	∞	90.0000	∞	π	0.0000	∞	---	0.0000	30.0000
	0.1000	0.9251	78.5000	0.4990	35.8000	71.5500	121.0000	3.1600	0.0666	499.0000	0.2510	0.0000	30.0000
	0.2000	0.8242	91.5000	0.5000	16.0000	58.5100	58.7000	3.0400	0.1310	260.0000	0.2490	0.1000	30.0000
	0.4000	0.6074	109.0000	0.5000	5.2000	41.0100	24.5000	2.5700	0.2360	136.0000	0.2420	0.5000	30.0000
	0.6000	0.4000	119.8000	0.5010	1.6500	30.1400	11.2000	1.9800	0.3460	86.1000	0.2280	1.5000	30.0000
	0.8000	0.2000	128.3000	0.5000	0.3330	21.7000	4.2700	1.3000	0.4960	54.9000	0.1950	3.2000	30.0000
	0.9000	0.1000	133.1000	0.5000	0.0844	16.8700	2.0100	0.8940	0.6200	41.0000	0.1590	4.3000	23.7000
	0.9700	0.0300	139.2000	0.5000	0.0110	10.8100	0.7130	0.5070	0.7860	29.1000	0.1070	4.1000	15.9000
	1.0000	0.0000	150.0000	0.5000	0.0000	0.0000	0.0000	---	1.0000	0.0000	0.0000	0.0000	0.0000

7. The ratio of average pressure to maximum pressure, P/p_{max}, in the fluid film as a function of Sommerfeld number is given in Fig. 8-7.
8. The location of the point of maximum pressure is given in Fig. 8-8. It is measured in degrees from the line along the load direction as shown in Fig. 8-8.
9. The location of the point of the end of the pressure wave is given in Fig. 8-9. It is measured in degrees from the line along the load direction as shown in Fig. 8-9. This is the angle θ_2 in this text, and it is referred to as θ_{p° in the chart of Raimondi and Boyd.
10. Curves of the minimum film thickness ratio, h_n/C as a function of the bearing arc, β (Deg.), are presented in Fig. 8-10 for two cases: a. maximum load capacity, b. minimum power losses due to friction. These curves are useful for the design engineer for selecting the optimum bearing arc, β, based on the requirement of maximum load capacity, or minimum power loss due to viscous friction.

Note that the preceding performance parameters are presented by graphs only for journal bearings with the ratio $L/D = 1$. For bearings having different L/D ratios, the performance parameters are listed in tables.

In Fig. 8-1 (chart 1), curves are presented of the film thickness ratio, h_n/C, versus the Sommerfeld number, S for various bearing arcs β. The curves for $\beta = 180^\circ$ and $\beta = 360^\circ$ nearly coincide. This means that for an identical bearing load, a full bearing ($\beta = 360^\circ$) does not result in a significantly higher value of h_n in comparison to a partial bearing of $\beta = 180^\circ$. This means that for an identical h_n, a full bearing ($\beta = 360^\circ$) does not have a much higher load capacity than a partial bearing. At the same time, it is clear from Fig. 8-3 (chart 3) that lowering the bearing arc, β, results in a noticeable reduction in the bearing friction (viscous friction force is reduced because of the reduction in oil film area).

In conclusion, the advantage of a partial bearing is that it can reduce the friction coefficient of the bearing without any significant reduction in load capacity (this advantage is for identical geometry and viscosity in the two bearings). In fact, the advantage of a partial bearing is more than indicated by the two figures, because it has a lower fluid film temperature due to a faster oil circulation. This improvement in the thermal characteristics of a partial bearing in comparison to a full bearing is considered an important advantage, and designers tend to select this type for many applications.

8.5 FLUID FILM TEMPERATURE

8.5.1 Estimation of Temperature Rise

After making the basic decisions concerning the bearing dimensions, bearing arc, and determination of the minimum film thickness h_n, the lubricant is selected. At this stage the bearing temperature is unknown, and it should be estimated. We assume an average bearing temperature and select a lubricant that would provide the required bearing load capacity (equal to the external load). The next step is to determine the flow rate of the lubricant in the bearing, Q, in the axial direction. Knowledge of this flow rate allows one to determine the temperature rise inside the fluid film from the charts. This will allow one to check and correct the initial assumptions made earlier concerning the average oil film temperature. Later, it is possible to select another lubricant for the desired average viscosity, based on the newly calculated temperature. A few iterations are required for estimation of the average temperature.

The temperature inside the fluid film increases as it flows inside the bearing, due to high shear rate flow of viscous fluid. The energy loss from viscous friction is dissipated in the oil film in the form of heat. There is an energy balance, and a large part of this heat is removed from the bearing by continuous convection as the hot oil flows out and is replaced by a cooler oil that flows into the bearing clearance. In addition, the heat is transferred by conduction through the sleeve into the bearing housing. The heat is transferred from the housing partly by convection to the atmosphere and partly by conduction through the base of the housing to the other parts of the machine. In most cases, precise heat transfer calculations are not practical, because they are too complex and because many parameters, such as contact resistance between the machine parts, are unknown.

For design purposes it is sufficient to estimate the temperature rise of the fluid ΔT, from the point of entry into the bearing clearance (at temperature T_{in}) to the point of discharge from the bearing (at temperature $T_{\max}$). This estimation is based on the simplified assumptions that it is possible to neglect the heat conduction through the bearing material in comparison to the heat removed by the continuous replacement of fluid. In fact, the heat conduction reduces the temperature rise; therefore, this assumption results in a design that is on the safe side, because the estimated temperature rise is somewhat higher than in the actual bearing. The following equation for the temperature rise of oil in a journal bearing, ΔT, was presented by Shigley and Mitchell (1983):

$$\Delta T = \frac{8.3P(f\,R/C)}{10^6\left(\dfrac{Q}{nRCL}\right)(1 - 0.5Q_s/Q)} \tag{8-5}$$

where ΔT is the temperature rise [°C], $P = F/2RL$ [Pa]. All the other parameters required for calculation of the temperature rise are dimensionless parameters.

They can be obtained directly from the charts or tables of Raimondi and Boyd as a function of the Sommerfeld number and L/D ratio. The average temperature in the fluid film is determined from the temperature rise by the equation

$$T_{av} = \frac{T_{in} + T_{max}}{2} = T_i + \frac{\Delta T}{2} \tag{8-6}$$

Equation (8-5) is derived by assuming that all the heat that is generated by viscous shear in the fluid film is dissipated only in the fluid (no heat conduction through the boundaries). This heat increases the fluid temperature. In a partial bearing, the maximum temperature is at the outlet at the end of the bearing arc. In a full bearing, the maximum temperature is after the minimum film thickness at the end of the pressure wave (angle θ_2). The mean temperature of the fluid flowing out, in the axial direction, Q, has been assumed as T_{av}, the average of the inlet and outlet temperatures.

Example Problem 8-1

Calculation of Temperature Rise

A partial journal bearing ($\beta = 180^\circ$) has a radial load $F = 10{,}000$ N. The speed of the journal is $N = 6000$ RPM, and the viscosity of the lubricant is 0.006 N-s/m^2. The geometry of the bearing is as follows:

Journal diameter: $D = 40$ mm
Bearing length: $L = 10$ mm
Bearing clearance: $C = 30 \times 10^{-3}$ mm

a. Find the following performance parameters:

Minimum film thickness h_n
Friction coefficient f
Flow rate Q
Axial side leakage Q_s
Rise in temperature ΔT if you ignore the heat conduction through the sleeve and journal

b. Given an inlet temperature of the oil into the bearing of 20°C, find the maximum and average temperature of the oil.

Solution

This example is calculated from Eq. (8-5) in SI units.

The bearing data is given by:

$$\beta = 180^\circ$$
$$\frac{L}{D} = \frac{1}{4}$$
$$P = \frac{F}{LD} = 25 \times 10^6 \text{ Pa}$$
$$n = \frac{6000}{60} = 100 \text{ rPS}$$

The Sommerfeld number [using Eq. (8-1)] is:

$$S = \left(\frac{2 \times 10^{-2}}{30 \times 10^{-6}}\right)^2 \frac{0.006 \times 100}{25 \times 10^6} = 0.0106$$

a. Performance Parameters

From the table for a $\beta = 180^\circ$ bearing) and $L/D = 1/4$, the following operating parameters can be obtained for $S = 0.0106$, the calculated Sommerfeld number.

Minimum Film Thickness:

$$\frac{h_n}{C} = 0.03 \qquad h_n = 0.9 \times 10^{-3} \text{ mm}$$

If the minimum film thickness obtained is less than the design value, the design has to modified.

Coefficient of Friction: The coefficient of friction is obtained from the table:

$$\frac{R}{C} f = 0.877 \qquad f = 0.0013$$

Flow rate:

$$\frac{Q}{nRCL} = 3.29 \qquad Q = 1.974 \times 10^{-6} \text{ m}^3/\text{s}$$

Side Leakage:

$$\frac{Q_s}{Q} = 0.961 \qquad Q_s = 1.897 \times 10^{-6} \text{ m}^3/\text{s}$$

Temperature Rise ΔT: The estimation of the temperature rise is based on Eq. (8-5) in SI units. The dimensionless operating parameters, from the appro-

priate table of Raimondi and Boyd, are substituted:

$$P = 25 \times 10^6 \text{ Pa} \qquad \left(1 - 0.5\frac{Q_s}{Q}\right) = 0.5195 \qquad \frac{R}{C}f = 0.877$$

$$\Delta T_m = \frac{8.3P[R/C(f)]}{10^6\left(\dfrac{Q}{nRCL}\right)[1 - (0.5)Q_s/Q]} = \frac{8.3 \times 25 \times 0.877}{3.29 \times 0.5195} = 106^\circ\text{C}$$

b. Maximum and Average Oil Temperatures:

Maximum temperature:

$$T_{\max} = T_{\text{in}} + \Delta T = 20 + 106 = 123^\circ\text{C}$$

Average temperature:

$$T_{\text{av}} = T_{\text{in}} + \frac{\Delta T}{2} = 20 + \frac{106}{2} = 73^\circ\text{C}$$

Since the bearing material is subjected to the maximum temperature of 123°C, the bearing material that is in contact with the lubricant should be resistant to this temperature. Bearing materials are selected to have a temperature limit well above the maximum temperature in the fluid film.

For bearing design, the Sommerfeld number, S, is determined based on lubricant viscosity at the average temperature of 73°C.

8.5.2 Temperature Rise Based on the Tables of Raimondi and Boyd

The specific heat and density of the lubricant affect the rate of heat transfer and the resulting temperature rise of the fluid film. However, Eq. (8-5) does not consider the properties of the lubricant, and it is an approximation for the properties of mineral oils. For other fluids, such as synthetic lubricants, the temperature rise can be determined more accurately from a table of Raimondi and Boyd. The advantage of the second method is that it can accommodate various fluid properties. The charts and tables include a temperature-rise variable as a function of the Sommerfeld number. The temperature-rise variable is a dimensionless ratio that includes the two properties of the fluid: the specific heat, c (Joule/kg-°C), and the density, ρ (kg/m^3). Table 8-5 lists these properties for engine oil as a function of temperature.

The following two problems illustrate the calculation of the temperature rise, based on the charts or tables of Raimondi and Boyd. The two examples involve calculations in SI units and Imperial units.* We have to keep in mind that

* The original charts of Raimondi and Boyd were prepared for use with Imperial units (the conversion of energy from BTU to lbf-inch units is included in the temperature-rise variable). In this text, the temperature-rise variable is applicable for any unit system.

TABLE 8-5 Specific Heat and Density of Engine Oil

Temperature, T		Specific heat, c		Density, ρ	
°F	°C	J/kg-°C	BTU/lb_m-°F	kg/m^3	lbm/ft^3
32	0	1796	0.429	899.1	56.13
68	20	1880	0.449	888.2	55.45
104	40	1964	0.469	876.1	54.69
140	60	2047	0.489	864.0	53.94
176	80	2131	0.509	852.0	53.19
212	100	2219	0.529	840.0	52.44
248	120	2307	0.551	829.0	51.75
284	140	2395	0.572	816.9	50.99
320	160	2483	0.593	805.9	50.31

both solutions are adiabatic, in the sense that the surfaces of the journal and the bearing are assumed to be ideal insulation. In practice, it means that conduction of heat through the sleeve and journal is disregarded in comparison to the heat taken away by the fluid. In this way, the solution is on the safe side, because it predicts a higher temperature than in the actual bearing.

Example Problem 8-2

Calculation of Transformation Rise in SI Units

Solve for the temperature rise ΔT for the journal bearing in Example Problem 8-1. Use the temperature-rise variable according to the Raimondi and Boyd tables and solve in SI units. Use Table 8-5 for the oil properties. Assume that the properties can be taken as for engine oil at 80°C

Solution

The temperature rise is solved in SI units based on the tables of Raimondi and Boyd. The properties of engine oil at 80°C are:

Specific heat (from Table 8-5): $c = 2131$ [Joule/kg-°C]
Density of oil (from Table 8-5): $\rho = 852$ [kg/m^3]
Bearing average pressure (see Example Problem 8-1): $P = 25 \times 10^6$ [N/m^2]
Temperature-rise variable (from Table 8-2 for $\beta = 180°$) is 6.46.

The equation is

$$\frac{c\rho}{P}\Delta T = 6.46$$

The properties and P are given, and the preceding equation can be solved for the temperature rise:

$$\Delta T = 6.46\frac{P}{c\rho} = 6.46\frac{25 \times 10^6}{2131 \times 852} = 88.9^{\circ}\text{C}$$

This temperature rise is considerably lower than that obtained by the equation of Shigley and Mitchell (1983) in Example Problem 8-1.

Example Problem 8-3

Calculation of Temperature Rise in Imperial Units

Solve for the temperature rise ΔT of the journal bearing in Example Problem 8-1. Use the temperature-rise variable according to the Raimondi and Boyd tables and solve in Imperial units. Use Table 8-5 for the oil properties. Assume that the properties can be taken as for engine oil at 176°F (equal to 80°C in Example Problem 8-2).

Solution

The second method is to calculate ΔT from the tables of Raimondi and Boyd in Imperial units. The following values are used:

Density of engine oil (at 176°F, from Table 8-1): $\rho = 53.19$ [lbm/ft^3] = $53.19/12^3 = 0.031$ [lbm/in^3.]
Specific heat of oil (from Table 8-5): $c = 0.509$ [BTU/lbm-F°]
Mechanical equivalent of heat: $J = 778$ [lbf-ft/BTU] = 778×12 [lbf-inch/BTU]

This factor converts the thermal unit BTU into the mechanical unit lbf-ft:

$$c = 0.509\ [\text{BTU/lbm} - {}^{\circ}\text{F}] \times 778 \times 12\ [\text{lbf-inch/BTU}]$$
$$= 4752\ [\text{lbf-inch/lbm} - \text{F}^{\circ}]$$

The bearing average pressure (from Example Problem 8-1):

$$P = 2.5 \times 10^6\ \text{Pa} = (25 \times 10^6)/6895 = 3626\ [\text{lbf/in}^2.]$$

The data in Imperial units results in a dimensionless temperature-rise variable where the temperature rise is in °F.

Based on the table of Raimondi and Boyd, the same equation is applied as in Example Problem 8-2:

$$\frac{c\rho}{P}\Delta T = 6.46$$

Solving for the temperature rise:

$$\Delta T = 6.46\frac{P}{c\rho} = 6.46\frac{3626}{4752 \times 0.031} = 159^\circ\text{F}$$

$$\Delta T = 147.7^\circ\text{F} \times \frac{5}{9}\ (^\circ\text{C}/^\circ\text{F}) = 88.3^\circ\text{C}$$

(close to the previous solution in SI units)

Note: The reference 32°F does not play a role here because we solve for the temperature difference, ΔT.

8.5.3 Journal Bearing Design

Assuming an initial value for viscosity, the rise in temperature, ΔT, is calculated and an average temperature of the fluid film is corrected. Accordingly, after using the calculated average temperature, the viscosity of the oil can be corrected. The new viscosity is determined from the viscosity–temperature chart (Fig. 2-3). The inlet oil temperature to the bearing can be at the ambient temperature or at a higher temperature in central circulating systems.

If required, the selection of the lubricant may be modified to account for the new temperature. In the next step, the Sommerfeld number is modified for the corrected viscosity of the previous oil, but based on the new temperature. Let us recall that the Sommerfeld number is a function of the viscosity, according to Eq. (8-1). If another oil grade is selected, the viscosity of the new oil grade is used for the new Sommerfeld number. Based on the new Sommerfeld number S, the calculation of Q and the temperature rise estimation ΔT are repeated. These iterations are repeated until there is no significant change in the average temperature between consecutive iterations. If the temperature rise is too high, the designer can modify the bearing geometry.

After the average fluid film temperature is estimated, it is necessary to select the bearing material. Knowledge of the material properties allows one to test whether the allowable limits are exceeded. At this stage, it is necessary to calculate both the peak pressure and the peak temperature and to compare those values with the limits for the bearing material that is used. The values of the maximum pressure and temperature rise in the fluid film are easy to determine from the charts or tables of Raimondi and Boyd.

8.5.4 Accurate Solutions

For design purposes, the average temperature of the fluid-film can be estimated as described in the preceding section. Temperature estimation is suitable for most practical cases. However, in certain critical applications, more accurate analysis is

required. The following is a general survey and references that the reader can use for advanced study of this complex heat transfer problem.

In a fluid film bearing, a considerable amount of heat is generated by viscous friction, which is dissipated in the oil film and raises its temperature. The fluid film has a non-uniform temperature distribution along the direction of motion (x direction) and across the film (z direction). The peak fluid film temperature is near the point of minimum film thickness. The rise in the oil temperature results in a reduction of the lubricant viscosity; in turn, there is a significant reduction of the hydrodynamic pressure wave and load carrying capacity. Accurate solution of the temperature distribution in the fluid film includes heat conduction through the bearing material and heat convection by the oil. This solution requires a numerical analysis, and it is referred to as a full *thermohydrodynamic* (THD) analysis. This analysis is outside the scope of this text, and the reader is referred to available surveys, such as by Pinkus (1990) and by Khonsari (1987). The results are in the form of isotherms mapping the temperature distribution in the sleeve. An example is included in Chap. 18.

8.6 PEAK TEMPERATURE IN LARGE, HEAVILY LOADED BEARINGS

The maximum oil film temperature of large, heavily loaded bearings is higher than the outlet temperature. Heavily loaded bearings have a high eccentricity ratio, and at high speed they are subjected to high shear rates and much heat dissipation near the minimum film thickness. For example, in high-speed turbines having journals of the order of magnitude of 10 in. (250 mm) and higher, it has been recognized that the maximum temperature near the minimum film thickness, h_n, is considerably higher than $T_{\text{in}} + \Delta T$, which has been calculated in the previous section. In bearings made of white metal (babbitt), it is very important to limit the maximum temperature to prevent bearing failure.

In a bearing with a white metal layer on its surface, creep of this layer can initiate at temperatures above 260°F. The risk of bearing failure due to local softening of the white metal is high for large bearings operating at high speeds and small minimum film thickness. Plastic bearings can also fail due to local softening of the plastic at elevated temperatures. The peak temperature along the bearing surface is near the minimum film thickness, where there is the highest shear rate and maximum heat dissipation by viscous shear. This is exacerbated by the combination of local high oil film pressure and high temperature at the same point, which initiates an undesirable creep process of the white metal. Therefore, it is important to include in the bearing design an estimation of the peak temperature near the minimum film thickness (in addition to the temperature rise, ΔT).

The yield point of white metals reduces significantly with temperature. The designer must ensure that the maximum pressure does not exceed its limit. If the temperature is too high, the designer can use bearing material with a higher melting point. Another alternative is to improve the cooling by providing faster oil circulation by means of several oil grooves. An example is the three-lobe bearing that will be described in Chapter 9.

Adiabatic solutions were developed by Booser et al. (1970) for calculating the maximum temperature, based on the assumption that the heat conduction through the bearing can be neglected in comparison to the heat removed by the flow of the lubricant. This assumption is justified in a finite-length journal bearing, where the axial flow rate has the most significant role in heat removal.

The derivation of the maximum temperature considers the following viscosity–temperature relation:

$$\mu = kT^{-n} \tag{8-7}$$

where the constants k and n are obtained from the viscosity–temperature charts. The viscosity is in units of lb-s/in^2. and the temperature is in deg. F.

The maximum temperatures obtained according to Eq. (8-8) were experimentally verified, and the computation results are in good agreement with the measured temperatures. The equation for the maximum temperature, $T_{\max}$, is (Booser et al., 1970):

$$T_{\max}^{n+1} - T_1^{n+1} = \frac{4\pi k(n+1)N}{60\rho c_p}\left(\frac{R}{C}\right)^2 \Delta G_j \tag{8-8}$$

Here, ρ is the lubricant density and c_p is its specific heat at constant pressure. The temperatures T_m and T_1 are the maximum and inlet temperatures, respectively. The temperatures, in deg. F, have an exponent of $(n+1)$ from the viscosity–temperature equation (8-7). The journal speed N is in revolutions per minute. The coefficient ΔG_j is a temperature-rise multiplier. It can be obtained from Fig. 8-11. It shows the rapid increase of ΔG_j at high eccentricity ratios ($\varepsilon = 0.8$–0.9), indicating that the maximum temperature is highly dependent on the film thickness, particularly under high loads.

For turbulent fluid films, the equation is

$$T_{\max} - T_1 = \frac{f\pi^2 N^2 D^3}{2gc_p(1-\varepsilon^2)}(\pi - \theta_1) \tag{8-9}$$

where f is the friction coefficient, D is the journal diameter, and g is gravitational acceleration, 386 in./s^2. The angle θ_1 is the oil inlet angle (in radians). The

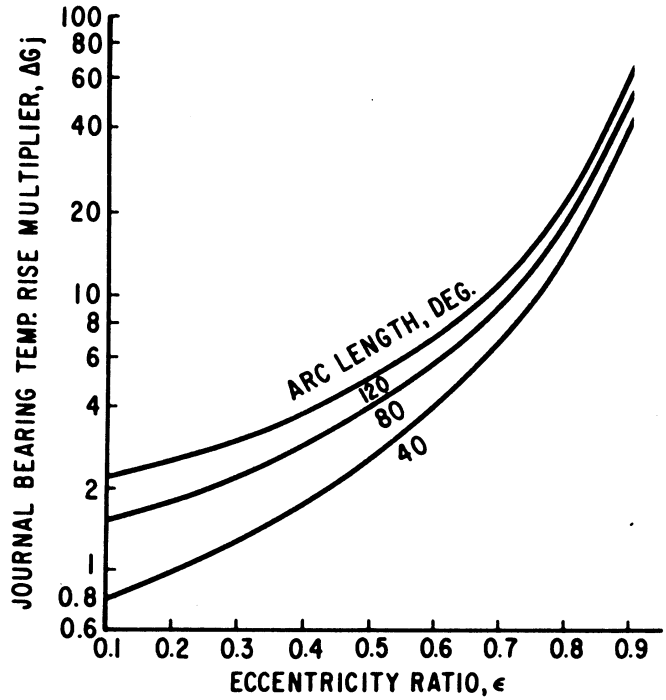

FIG. 8-11 Journal bearing temperature-rise multiplier for Eq. (8-8). (From Booser et al., 1970, with permission of STLE.)

friction coefficient is determined by experiment or taken from the literature for a similar bearing.

8.7 DESIGN BASED ON EXPERIMENTAL CURVES

In the preceding discussion, it was shown that the complete design of hydrodynamic journal bearings relies on important decisions: determination of the value of the minimum film thickness, h_n, and the upper limit of bearing operating temperature. The minimum value of h_n is determined by the surface finish of the bearing and the journal as well as other operating conditions that have been discussed in this chapter. However, the surface finish may vary after running the machine, particularly for the soft white metal that is widely used as bearing material. In addition to the charts of Raimondi and Boyd, which are based on hydrodynamic analysis, bearing design engineers need design tools that are based

on previous experience and experiments. In particular for bearing design for critical applications, there is a merit in also relying on experimental curves for determining the limits of safe hydrodynamic performance.

In certain machines, there are design constraints that make it necessary to have highly loaded bearings operating with very low minimum film thickness. Design based on hydrodynamic theory is not very accurate for highly loaded bearings at very thin h_n. The reason is that in such cases, it is difficult to predict the temperature rise, ΔT, and the h_n that secure hydrodynamic performance. In such cases, the limits of hydrodynamic bearing operation can be established only by experiments or experience with similar bearings. There are many examples of machines that are working successfully with hydrodynamic bearings having much lower film thickness than usually recommended.

For journal bearings operating in the full hydrodynamic region, the friction coefficient, f, is an increasing function of the Sommerfeld number. Analytical curves of $(R/C)f$ versus the Sommerfeld number are presented in the charts of Raimondi and Boyd; see Fig. 8-3. These curves are for partial and full journal bearings, for various bearing arcs, β. Of course, the designer would like to operate the bearing at minimum friction coefficient. However, these charts are only for the hydrodynamic region and do not include the boundary and mixed lubrication regions. These curves do not show the lowest limit of the Sommerfeld number for maintaining a full hydrodynamic film. A complete curve of $(R/C)f$ versus the Sommerfeld number over the complete range of boundary, mixed, and hydrodynamic regions can be obtained by testing the bearing friction against variable speed or variable load. These experimental curves are very helpful for bearing design. Description of several friction testing systems is included in Chapter 14.

8.7.1 Friction Curves

The friction curve in the boundary and mixed lubrication regions depends on the material as well as on the surface finish. For a bearing with constant C/R ratio, the curves of $(R/C)f$ versus the Sommerfeld number, S, can be reduced to dimensionless, experimental curves of the friction coefficient, f, versus the dimensionless ratio, $\mu n/P$. These experimental curves are very useful for design purposes. In the early literature, the notation for viscosity is z, and the variable zN/P has been widely used. In this text, the ratio $\mu n/P$ is preferred, because it is dimensionless and any unit system can be used as long as the units are consistent. In addition, this ratio is consistent with the definition of the Sommerfeld number.

The variable zN/P is still widely used, because it is included in many experimental curves that are provided by manufacturers of bearing materials. Curves of f versus zN/P are often used to describe the performance of a specific

bearing of constant geometry and material combination. This ratio is referred to as the Hersey* number. The variable zN/P is not completely dimensionless, because it is used as a combination of Imperial units with metric units for the viscosity. The average pressure is in Imperial units [psi], the journal speed, N, is in revolutions per minute [RPM], and the viscosity, z, is in centipoise. In order to have dimensionless variables, the journal speed, n, must always be in revolutions per second (RPS), irrespective of the system of units used, and the viscosity, μ, must always include seconds as the unit of time. The variable zN/P is proportional and can be converted to the dimensionless variable $\mu n/P$.

Transition from Mixed to Hydrodynamic Lubrication

A typical experimental curve of the friction coefficient, f, versus the dimensionless variable, $\mu n/P$, is shown in Fig. 8-12. The curve shows the region of hydrodynamic lubrication, at high values of $\mu n/P$, and the region of mixed

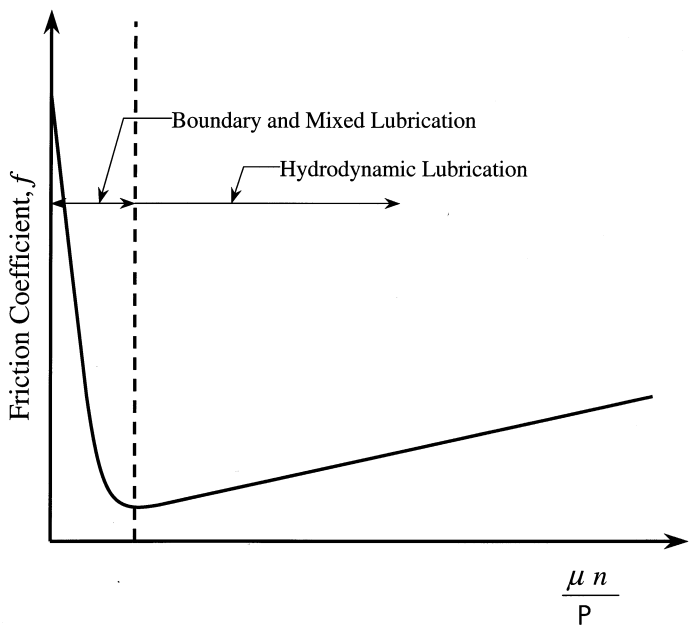

FIG. 8-12 Friction coefficient, f, versus variable $\mu n/P$ in a journal bearing,

* After Mayo D. Hersey, for his contribution to the lubrication field.

lubrication, at lower values of $\mu n/P$. The transition point $(\mu n/P)_{tr}$ from mixed to hydrodynamic lubrication is at the point of minimum friction coefficient.

Hydrodynamic theory indicates that minimum film thickness increases with the variable $\mu n/P$. Full hydrodynamic lubrication is where $\mu n/P$ is above a certain transition value $(\mu n/P)_{tr}$. At the transition point, the minimum film thickness is equal to the size of surface asperities. However, in the region of full hydrodynamic lubrication, the minimum film thickness is higher than the size of surface asperities, and there is no direct contact between the sliding surfaces. Therefore, there is only viscous friction, which is much lower in comparison to direct contact friction. In the hydrodynamic region, viscous friction increases with $\mu n/P$, because the shear rates and shear stresses in the fluid film are increasing with the product of viscosity and speed.

Below the critical value $(\mu n/P)_{tr}$, there is mixed lubrication where the thickness of the lubrication film is less than the size of the surface asperities. Under load, there is direct contact between the surfaces, resulting in elastic as well as plastic deformation of the asperities. In the mixed region, the external load is carried partly by the pressure of the hydrodynamic fluid film and partly by the mechanical elastic reaction of the deformed asperities. The film thickness increases with $\mu n/P$; therefore, as the velocity increases, a larger portion of the load is carried by the fluid film. In turn, the friction decreases with $\mu n/P$ in the mixed region, because the fluid viscous friction is lower than the mechanical friction due to direct contact between the asperities. The transition value, $(\mu N/P)_{tr}$, is at the minimum friction, where there is a transition in the trend of the friction slope.

Design engineers are often tempted to design the bearing at the transition point $(\mu n/P)_{tr}$ in order to minimize friction-energy losses as well as to minimize the temperature rise in the bearing. However, a close examination of bearing operation indicates that it is undesirable to design at this point. The purpose of the following discussion is to explain that this point does not have the desired operation stability. The term *stability* is used here in the sense that the hydrodynamic operation would recover and return to normal operation after any disturbance, such as overload for a short period or unexpected large vibration of the machine. In contrast, unstable operation is where any such disturbance would result in deterioration in bearing operation that may eventually result in bearing failure.

Although it is important to minimize friction-energy losses, if the bearing operates at the point $(\mu N/P)_{tr}$, where the friction is minimal, any disturbance would result in a short period of higher friction. This would cause a chain of events that may result in overheating and even bearing failure. The higher friction would result in a sudden temperature rise of the lubricant film, even if the disturbance discontinues. Temperature rise would immediately reduce the fluid viscosity, and the magnitude of the variable $\mu n/P$ would decrease with the

viscosity. In turn, the bearing would operate in the mixed region, resulting in higher friction. The higher friction causes further temperature rise and further reduction in the value of $\mu n/P$. This can lead to an unstable chain reaction that may result in bearing failure, particularly for high-speed hydrodynamic bearings.

In contrast, if the bearing is designed to operate on the right side of the transition point, $\mu n/P > (\mu N/P)_{tr}$, any unexpected temperature rise would also reduce the fluid viscosity and the value of the variable $\mu n/P$. However in that case, it would shift the point in the curve to a lower friction coefficient. The lower friction would help to restore the operation by lowering the fluid film temperature. The result is that a bearing designed to operate at somewhat higher value of $\mu n/P$ has the important advantage of stable operation.

The decision concerning h_n relies in many cases on previous experience with bearings operating under similar conditions. In fact, very few machines are designed without any previous experience as a first prototype, and most designs represent an improvement on previous models. In order to gain from previous experience, engineers should follow several important dimensionless design parameters of the bearings in each machine. As a minimum, engineers should keep a record of the value of $\mu n/P$ and the resulting analytical minimum film thickness, h_n, for each bearing. Experience concerning the relationship of these variables to successful bearing operation, or early failure, is essential for future designs of similar bearings or improvement of bearings in existing machinery. However, for important applications, where early bearing failure is critical, bearing tests should be conducted *before* testing the machine in service. This is essential in order to prevent unexpected expensive failures. Testing machines will be discussed in Chapter 14.

Problems

8-1 Select the lubricant for a full hydrodynamic journal bearing ($\beta = 360^\circ$) under a radial load of 1 ton. The design requirement is that the minimum film thickness, h_n, during steady operation, not be less than 16×10^{-3} mm. The inlet oil temperature is 40°C, and the journal speed is 3600 RPM. Select the oil type that would result in the required performance. The bearing dimensions are: $D = 100$ mm; $L = 50$ mm, $C = 80 \times 10^{-3}$ mm.

Directions: First, determine the required Sommerfeld number, based on the minimum film thickness, and find the required viscosity. Second evaluate the temperature rise Δt and the average temperature, and select the oil type (use Fig. 2-2).

8-2 Use the Raimondi and Boyd charts to find the maximum load capacity of a full hydrodynamic journal bearing ($\beta = 360^\circ$). The

lubrication is SAE 10. The bearing dimensions are: $D = 50\,\text{mm}$, $L = 50\,\text{mm}$, $C = 50 \times 10^{-3}\,\text{mm}$. The minimum film thickness, h_n, during steady operation, should not be below $10 \times 10^{-3}\,\text{mm}$. The inlet oil temperature is 30°C and the journal speed is 6000 RPM.

Directions: Trial-and-error calculations are required for solving the temperature rise. Assume a temperature rise and average temperature. Find the viscosity for SAE 10 as a function of temperature, and use the chart to find the Sommerfeld number and the resulting load capacity. Use the new average pressure to recalculate the temperature rise. Repeat iterations until the temperature rise is equal to that in the previous iteration.

8-3 The dimensions of a partial hydrodynamic journal bearing, $\beta = 180°$, are: $D = 60\,\text{mm}$, $L = 60\,\text{mm}$, $C = 30 \times 10^{-3}\,\text{mm}$. During steady operation, the minimum film thickness, h_n, should not go below $10 \times 10^{-3}\,\text{mm}$. The maximum inlet oil temperature (in the summer) is 40°C, and the journal speed is 7200 RPM. Given a lubricant of SAE 10, use the chart to find the maximum load capacity and the maximum fluid film pressure, $p_{\max}$.

8-4 A short journal bearing is loaded by 500 N. The journal diameter is 25 mm, the L/D ratio is 0.6, and $C/R = 0.002$. The bearing has a speed of 600 RPM. An experimental curve of friction coefficient, f, versus variable $\mu n/P$ of this bearing is shown in Fig. 8-12. The minimum friction is at $\mu n/P = 3 \times 10^{-8}$.

a. Find the lubrication viscosity for which the bearing would operate at a minimum friction coefficient.
b. Use infinitely-short-bearing theory and find the minimum film thickness at the minimum-friction point.
c. Use the charts of Raimondi and Boyd to find the minimum film thickness at the minimum-friction point.
d. For stable bearing operation, increase the variable $\mu n/P$ by 20% and find the minimum film thickness and new friction coefficient. Use the short bearing equations.